



HAL
open science

Highly confining planar proton exchanged waveguides on z-cut LiNbO₃ without degrading its nonlinear coefficients: the HISoPE process

Oleksandr Stepanenko, Emmanuel Quillier, Hervé Tronche, Pascal Baldi,
Marc de Micheli

► To cite this version:

Oleksandr Stepanenko, Emmanuel Quillier, Hervé Tronche, Pascal Baldi, Marc de Micheli. Highly confining planar proton exchanged waveguides on z-cut LiNbO₃ without degrading its nonlinear coefficients: the HISoPE process. IEEE Photonics Technology Letters, 2014, pp.1557. hal-01074550

HAL Id: hal-01074550

<https://hal.science/hal-01074550>

Submitted on 14 Oct 2014

HAL is a multi-disciplinary open access archive for the deposit and dissemination of scientific research documents, whether they are published or not. The documents may come from teaching and research institutions in France or abroad, or from public or private research centers.

L'archive ouverte pluridisciplinaire **HAL**, est destinée au dépôt et à la diffusion de documents scientifiques de niveau recherche, publiés ou non, émanant des établissements d'enseignement et de recherche français ou étrangers, des laboratoires publics ou privés.

Highly confining planar proton exchanged waveguides on z-cut LiNbO₃ without degrading its nonlinear coefficients: the HISoPE process.

Oleksandr Stepanenko, Emmanuel Quillier, Hervé Tronche, Pascal Baldi, and Marc De Micheli

Abstract—We propose a new proton exchange process to reproducibly realize on lithium niobate highly confining ($\delta n_e = 0.1$) planar waveguides without degrading the nonlinear coefficient of the crystal. Waveguides were fabricated with different acidic baths and the crystallographic changes, the index profiles and the local SHG response were measured. We show that for certain fabrications conditions, characteristic of the so-called High Index Soft Proton Exchange process (HISoPE), the high index modification can be obtained without degrading the crystal nonlinear coefficient. This result should open the way to the fabrication of very efficient nonlinear devices.

Index Terms—waveguide, lithium niobate, integrated optics, proton exchange, nonlinear optics.

I. INTRODUCTION

LITHIUM Niobate (LN) is known and widely used in integrated optics for its high nonlinear and electro-optic coefficients. Commercial devices are based on two fabrication techniques: the Ti-indiffusion [1], [2], which allows obtaining very low losses for telecom modulators at $1.5\ \mu\text{m}$, and the Annealed Proton Exchange (APE) process [3], which allows fabricating waveguides with a high polarization rejection and a better resistance to the optical damage, for applications using a shorter wavelength. In the labs, to improve the nonlinear efficiency, people have used Soft Proton Exchange (SPE) and Reverse Proton Exchange waveguides, which allow improving the confinement by respectively showing a slightly higher index increase or a symmetric index profile. All these techniques induce no or very small modifications of the crystallographic properties and are not affecting the electro-optics and nonlinear properties of the crystal but lead to gradient index profile waveguides with low index increase δn_e (between 0.01 and 0.03).

Nowadays no LN device is using the most confining waveguides presenting a step index profile with the highest $\delta n_e=0.1$ reported so far [4]. Indeed such waveguides are obtained when the proton exchange is performed in pure acid (generally benzoic acid) heated between 200 and 300°C and in this case the nonlinear coefficients are totally degraded [5]. Such waveguides are called PE waveguides in this paper.

Up to now, Vapor-phase Proton Exchange (VPE) is the only technique that proposed the possibility to combine a strong confinement ($\delta n_e=0.09$) with preserved nonlinearities [6]. However, the control of the fabrication conditions of VPE

waveguides is rather complicated, which results in its very poor reproducibility [7] and explains the fact that no functional device realized by VPE has been reported yet.

In this paper we present a new waveguide fabrication technique on LN, which allows combining a high optical confinement with $\delta n_e \geq 0.09$, undegraded nonlinear coefficient and a good reproducibility. We call this process HISoPE for High Index Soft Proton Exchange.

II. FABRICATION OF THE WAVEGUIDES

In order to compare the properties of the HISoPE waveguides with those of the other members of the PE family, APE, SPE, etc., a set of planar waveguides was fabricated on z-cut LN samples, cut from 3" Gooch & Housego Palo Alto, (formerly Crystal Technology) wafers using a diamond wire saw. As proton sources, we used benzoic acid (BA) melts buffered with lithium benzoate (LB) with $\rho_{LB} = m(LB)/[m(LB) + m(BA)]$ ranging from 0 to 3%. In order to limit the number of varying parameters, all the samples were processed at 300°C following the sealed ampules process [8] using an inert metallic container that stands the benzoic acid vapor pressure much better than the Pyrex ampules.

The container is filled with the BA+LB mixture in its bottom part and the samples to process are fixed in the upper one, evacuated down to a pressure of 3 mbar, which allows controlling the atmosphere in the container, and finally hermetically closed. Then it is placed into a furnace at 300°C and after 30 minutes, when both the melt and the samples have reached the exchange temperature, it is turned upside down, dipping the crystals into the melt and allowing the exchange to start. The exchange time can vary from several hours to several days depending on the aimed waveguide depth and the melt composition. When the exchange is finished the container is turned upside down again, allowed to cool and then open to get out the samples. In this work, we concentrated on samples produced with amounts of LB such that the working point is near but inferior to the threshold concentration $\rho_{th} = 2.7\%$ above which we obtain SPE waveguides at 300°C [4].

The samples were fabricated using the following values of ρ_{LB} : 0% to have a reference as a PE waveguide, 2.9% to have a reference as a SPE waveguide, and from 2% to 2.4% to have an indication of the range in which it is possible to produce HISoPE waveguides. Values below but near 2% have been shown to produce poor quality waveguides [4] and were not used. Values between 2.4% and 2.7% were also not used as

they are too close to $\rho_{th}\%$ for SPE and may lead to waveguides which are also of poor quality.

III. CRYSTALLOGRAPHIC CHARACTERIZATION BY X-RAY DIFFRACTION

The crystalline structure of the planar waveguides has been studied using X-Ray diffraction method, which allows measuring the modifications of the lattice parameters of the exchanged layer. We used the diffraction from the (00.12) planes parallel to the surface of the z-cut LN samples, which, in the substrate, is observed at the Bragg angle $\theta = 40.85^\circ$. This value is used as origin in the reported graphs (Fig.1), and in order to identify the obtained crystallographic phases, the diffraction spectra are compared to the ones reported in [9].

Structural characterizations show a clear difference between the PE, HISoPE and SPE waveguides. SPE waveguides are associated to a graded variation of the cell parameter, which is represented by a gradient extending down to an angle of $-150''$ indicating that all the waveguides is in the α phase (see Fig.1).

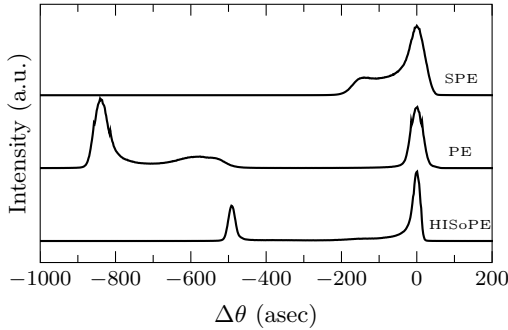


Fig. 1. Typical X-ray rocking curves of SPE, PE and HISoPE planar waveguides. The temperature of fabrication is the same for the three samples and is 300°C . Lithium benzoate concentration was $\rho_{LB} = 2.9\%$, 2.4% and 0% for SPE, HISoPE and PE waveguides, respectively.

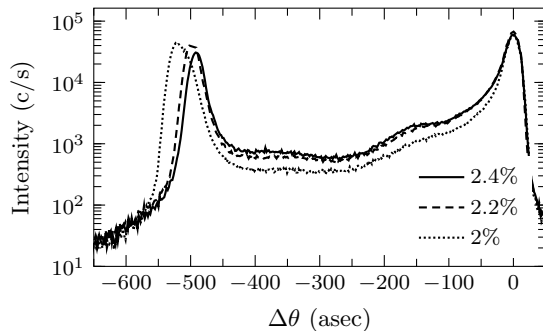


Fig. 2. Spectra of XRD from (00.12) planes of HISoPE planar waveguides. The characterized z-cut HISoPE waveguides were fabricated during 17 hour at 300°C and with different ρ_{LB} : 2% , 2.2% and 2.4% .

PE waveguiding layer is formed of two crystallographic phases, β_1 represented by a broad peak around $-580''$ and β_2 with a well defined peak at $-840''$. One has to note that the β_1 sublayer is not of the same crystalline quality as the β_2 sublayer. This may impact the optical properties. Note also that in this case, the lattice mismatch is very important

and therefore important strains and stresses are present in this kind of waveguides, and produce unwanted effects [10] in the devices fabricated using this recipe.

HISoPE waveguides exhibit one sharp intense peak with the same FWHM as the substrate peak indicating that the crystalline quality has not been affected by the process (see Fig.1). The position of this peak corresponds to the κ_2 phase. The substrate peak is no longer symmetric, and as for the SPE waveguides, a certain intensity can be seen down to an angle of $-150''$, which indicates that a small amount of the modified α phase is present in the waveguide. We can then expect a complex index profile with different sections associated to the different crystallographic layers. We can also note that the spectrum of the HISoPE waveguides are very similar to the X-ray rocking curves of the VPE waveguides [11] although the fabrication methods are completely different. At this stage of the characterization, similar nonlinear properties can be expected.

In this work we have let ρ_{LB} vary from 2 to 2.4%. The X-ray spectra (Fig.2) show that the cell modification increases when ρ_{LB} is reduced without any other dramatic change, which indicate that all the waveguides produced in this range of concentration are of the HISoPE type.

IV. INDEX PROFILE RECONSTRUCTION USING M-LINES MEASUREMENTS

The effective indices of the modes of the different waveguides have been measured using a two-prisms coupling technique [12] in order to evaluate their propagation losses and to reconstruct their index profiles. Light scattering along the propagation allows estimating the propagation losses. A typical value is < 1 dB/cm.

The index reconstruction is a two steps process. The first step consists in using the IWKB method [13], in order to evaluate the shape of the profile and the value of the depth and the index increase δn_e of the different layers. This step cannot give a precise estimation when the index profile contains a step index part but as soon as they are thick enough to support a mode at the characterization wavelength, the different layers are clearly identified.

The second step consists in calculating the effective indices of a waveguide with the obtained complex index profile shape and looking for the best fit with the measured values. This step is used to optimize the profile given by the IWKB method, without adding new layers.

PE waveguides are formed of two different crystallographic layers (β_1 and β_2 phases) but the index profile is a simple step. SPE waveguides (α phase) present a graded variation of the cell parameter and a graded index profile (Fig.4). For the HISoPE waveguides, we obtained a more complex index profile. The crystallographic characterizations indicate that there are two layers to take into account (Fig.2), one showing a well defined cell parameters modification (κ_2) and an other one very similar to the α phase layer observed for SPE waveguides. In the index profile, both layers are clearly identified and we took them into consideration to show that the κ_2 layer is responsible for the step part of the index profile

with a $\delta n_e = 0.1$ at $\lambda = 633$ nm, while the graded layer is well fitted with an exponential function as for SPE waveguides (Fig.3). It is worth noting that the values of the index increase involved in the profiles do not depend on ρ_{LB} .

An important parameter for a waveguide fabrication technique being the reproducibility we test it by realizing samples with the same fabrication parameters and performed index profile characterization. The results are reported in Fig.3, and show that the process is pretty well controlled.

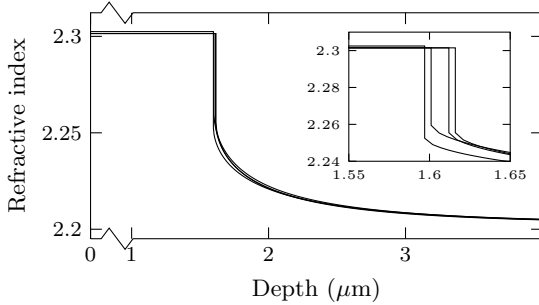


Fig. 3. Index profiles (at $\lambda = 633$ nm) of 4 planar HISoPE waveguides realized at the same conditions: 300°C in $\rho_{LB}=2\%$ melt during 17 hours. All the sample were fabricated at different time during the year.

V. SURFACE SHG RESPONSE

The local value of the d_{33} nonlinear coefficient was probed by surface SHG microscopy using the experimental set-up described in our previous works [14]. This setup, which has been improved and is now known as scanning SHG microscopy, is widely used to visualize domains in ferroelectric crystals [15]. A laser beam at 1.55 μm is focused on the polished end facets of the waveguides and scanned through the different layers: substrate, exchanged layers, air. This characterization technique permits to compare the value of the nonlinear coefficient in the waveguiding layers with its value in the substrate. The results are given in Figs.4-5. The intensities of the fundamental and the second harmonic are normalized by their maxima and plotted as a function of the waveguide depth. The index profiles are also plotted to see the correlations between the modifications of the index and of the nonlinear coefficient.

For the PE waveguide we obtain a SHG response that is strongly reduced in the exchanged layer (Fig.4). In other work, people have reported no signal in the exchanged layer, but it is worth to note that the waveguide tested here is fabricated at 300°C in a hermetically closed container while the other samples were fabricated at lower temperature in open containers. As we know from previous works on x-cut LN substrates, increasing the exchange temperature improves the crystalline quality of the exchanged layer [10], [16]. Some differences in the nonlinear response may be due to this difference in the fabrication conditions despite the index profiles are similar.

For the SPE waveguide (Fig.4), we see that the SH signal follows exactly the fundamental signal and as soon as the beam is completely focused in the material the SHG signal is constant showing no variation between the exchanged area and

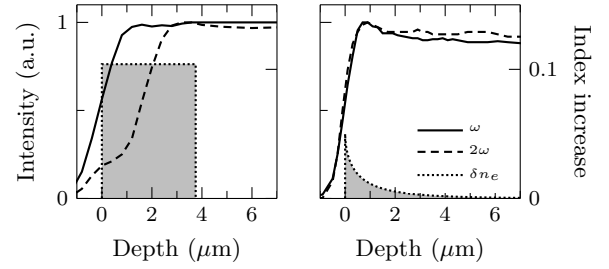


Fig. 4. Surface SHG profiling of PE (a) and SPE (b) waveguide and the corresponding index profiles (at $\lambda = 633$ nm). The samples were fabricated with $\rho_{LB} = 0\%$ at 360°C during 30 minutes for PE, and with $\rho_{LB} = 2.9\%$ at 300°C during 3 days for SPE.

the substrate. This indicates that the α layer presents the same nonlinear coefficient as the substrate, which has been verified in many other experiments using these nonlinear waveguides [17].

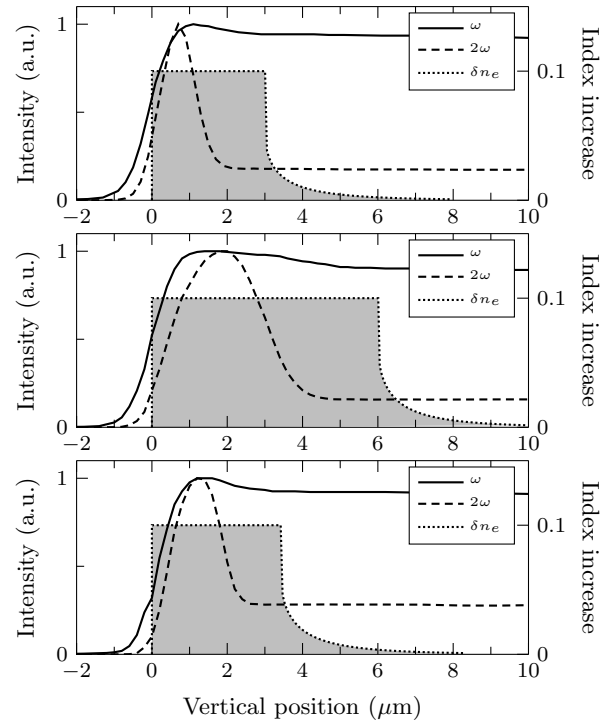


Fig. 5. Surface SHG profiling of HISoPE waveguides and their index profiles at $\lambda=633$ nm. The samples were fabricated using ρ_{LB} : (a) 2.4% during 35 hours; (b) 2.2% during 72 hours; (c) 2% during 40 hours. Fabrication temperature is 300°C.

It is worth to note that in these surface SHG experiments, one always observe a maximum of the SHG signal when the spot crosses an interface with a discontinuity of the d_{33} along the propagation direction [18]. This is related to the phase profile in the focused beam and the sign of the phase mismatch in the material. It is therefore very important to verify that during the scan the focus point is always at the same distance of the polished end face. This is proved by the fact that the SH signal is constant when the scan explore the substrate.

With the HISoPE waveguides (Fig.5), the SHG response shows a more or less sharp peak after the air-crystal interface

but no variation at the waveguide-substrate interface. The value of this maximum is probably affected by the index modification in the crystal and the associated guiding effect, despite in the experiments nothing is done to optimize the coupling into the waveguide. Therefore, without a careful modeling of the reflected SHG signal it is impossible to extract information about the exact value of the nonlinear coefficient near the surface but it is possible to say that d_{33} is not reduced as in the PE waveguides.

In [14], we also observed such a SHG peak with APE waveguides. We explained this peak by an extra backscattering coming from the bad quality of the produced waveguides. In this case the phenomena was also associated with a strong degradation of the retro-reflected fundamental beam, which was not observed with any of the samples we tested here. At the waveguide substrate interface, the absence of variation of the SH signal, allows saying that there is no variation of the d_{33} coefficient on the same area. Therefore, despite the presence of the SHG peak is difficult to explain, these results show that HISoPE process allows fabricating low loss planar waveguides in z-cut LN exhibiting a $\delta n_e = 0.1$ and no reduction of the nonlinear coefficient. This result is very important as it opens the way to the fabrication of very efficient nonlinear devices.

VI. CONCLUSION

In this paper we have presented a preliminary work aiming at fabricating highly confining waveguides on LN without destroying the nonlinear properties of the crystal. By measuring the crystallographic properties of the produced waveguides as well as their linear and nonlinear properties, we have shown that adding an appropriate amount of lithium benzoate in benzoic acid allows obtaining this result. This study confirms that very different layers can exhibit the same index profile, which can explain some “contradictions” reported in the literature, and show that there is a strong correlation between crystallographic and nonlinear properties. Finally, we have demonstrated that the HISoPE process, which produces highly confining planar waveguides with preserved nonlinearities, is quite reproducible what makes of him a good candidate to realize highly efficient nonlinear devices.

ACKNOWLEDGMENT

The authors would like to thank Maud Nemoz (CNRS-CRHEA, rue Bernard Grégory, 06560 VALBONNE, France) for her valuable contribution to this research providing a useful help in XRD characterizations.

REFERENCES

- [1] R. Schmidt and I. Kaminow, “Metal-diffused optical waveguides in LiNbO₃,” *Appl. Phys. Lett.*, vol. 25, no. 8, pp. 458–460, Oct 1974.
- [2] A. Neyer and W. Sohler, “High-speed cutoff modulator using a Ti-diffused LiNbO₃ channel waveguide,” *Appl. Phys. Lett.*, vol. 35, no. 3, pp. 256–258, 1979.
- [3] M. L. Bortz and M. M. Fejer, “Annealed proton-exchanged LiNbO₃ waveguides,” *Opt. Lett.*, vol. 16, no. 23, pp. 1844–1846, Dec 1991.
- [4] P. Baldi, M. P. De Micheli, K. El Hadi, S. Nouh, A. C. Cino, P. Aschieri, and D. B. Ostrowsky, “Proton exchanged waveguides in LiNbO₃ and LiTaO₃ for integrated lasers and nonlinear frequency converters,” *Op. Eng.*, vol. 37, no. 4, pp. 1193–1202, 1998.
- [5] F. Laurell, M. G. Roelofs, and H. Hsiung, “Loss of optical nonlinearity in proton-exchanged LiNbO₃ waveguides,” *Appl. Phys. Lett.*, vol. 60, no. 3, pp. 301–303, 1992.
- [6] J. Rams and J. M. Cabrera, “Preparation of proton-exchange LiNbO₃ waveguides in benzoic acid vapor,” *J. Opt. Soc. Am. B*, vol. 16, no. 3, pp. 401–406, Mar 1999.
- [7] L. Chanvillard, “Interactions paramétriques guidées de grande efficacité : utilisation de l’échange protonique doux sur niobate de lithium inverse périodiquement,” Ph.D. dissertation, Université Nice Sophia Antipolis, 1999.
- [8] M. Li, M. De Micheli, D. Ostrowsky, and M. Papuchon, “Réalisation sur LiNbO₃ de guides d’ondes présentant une forte variation d’indice et de très faibles pertes,” *Annales des Télécommunications*, vol. 43, no. 1–2, pp. 73–77, 1988.
- [9] Y. N. Korkishko, V. A. Fedorov, M. P. D. Micheli, P. Baldi, K. E. Hadi, and A. Leycuras, “Relationships between structural and optical properties of proton-exchanged waveguides on z-cut lithium niobate,” *Appl. Opt.*, vol. 35, no. 36, pp. 7056–7060, Dec 1996.
- [10] S. Chen, A. Leycuras, G. Tartarini, P. Bassi, P. Baldi, M. P. D. Micheli, and D. B. Ostrowsky, “Loss mechanisms and hybrid modes in high- δn_e proton-exchanged planar waveguides,” *Opt. Lett.*, vol. 18, no. 16, pp. 1314–1316, Aug 1993.
- [11] D. Tsou, M. Chou, P. Santhanaraghavan, Y. Chen, and Y. Huang, “Structural and optical characterization for vapor-phase proton exchanged lithium niobate waveguides,” *Mater. Chem. Phys.*, vol. 78, no. 2, pp. 474 – 479, 2003.
- [12] P. K. Tien and R. Ulrich, “Theory of prism-film coupler and thin-film light guides,” *J. Opt. Soc. Am.*, vol. 60, no. 10, pp. 1325–1337, Oct 1970.
- [13] J. M. White and P. F. Heidrich, “Optical waveguide refractive index profiles determined from measurement of mode indices: a simple analysis,” *Appl. Opt.*, vol. 15, no. 1, pp. 151–155, Jan 1976.
- [14] K. E. Hadi, M. Sundheimer, P. Aschieri, P. Baldi, M. P. D. Micheli, D. B. Ostrowsky, and F. Laurell, “Quasi-phase-matched parametric interactions in proton-exchanged lithium niobate waveguides,” *J. Opt. Soc. Am. B*, vol. 14, no. 11, pp. 3197–3203, Nov 1997.
- [15] S. A. Denev, T. T. A. Lummen, E. Barnes, A. Kumar, and V. Gopalan, “Probing ferroelectrics using optical second harmonic generation,” *J. Am. Ceram. Soc.*, vol. 94, no. 9, pp. 2699–2727, 2011.
- [16] M. De Micheli, D. Ostrowsky, J. Barety, C. Canali, A. Carnera, G. Mazzi, and M. Papuchon, “Crystalline and optical quality of proton exchanged waveguides,” *J. Lightwave Techn.*, vol. 4, no. 7, pp. 743–745, Jul 1986.
- [17] Y. Korkishko, V. Fedorov, and F. Laurell, “The SHG-response of different phases in proton exchanged lithium niobate waveguides,” *IEEE J. Sel. Top. Quant. Electron.*, vol. 6, no. 1, pp. 132–142, Jan 2000.
- [18] J. Kaneshiro, S. Kawado, H. Yokota, Y. Uesu, and T. Fukui, “Three-dimensional observations of polar domain structures using a confocal second-harmonic generation interference microscope,” *J. Appl. Phys.*, vol. 104, no. 5, pp. 054112–054112–7, Sep 2008.